On the Performance of Regenerative Relaying for SWIPT in NOMA Systems

Huu Q. Tran[1,2], Ca V. Phan[1], Quoc-Tuan Vien[3]
[1]Ho Chi Minh City University of Technology and Education, Vietnam.
Email: ttdv08@gmail.com/huutq.ncs@hcmute.edu.vn; capv@hcmute.edu.vn
[2]Industrial University of Ho Chi Minh City, Vietnam. Email: tranquyhuu@iuh.edu.vn
[3]Middlesex University, United Kingdom. Email: q.vien@mdx.ac.uk

***Abstract*—As a potential access strategy in 5G mobile communication systems, non-orthogonal multiple access (NOMA) has been proposed as a supplement to the traditional orthogonal multiple access (OMA). This paper investigates simultaneous wireless information and power transfer (SWIPT) in a NOMA relaying system. The data is transferred from a source to two end terminals among which the one close to the source acts as a relay employing decode-and-forward protocol to assist the far-end one. In order to simultaneously harvest the energy and information processing at relay node, power-splitting relaying (PSR) and time switching-based relaying (TSR) protocols are sequentially considered. Outage probability and ergodic rate of both protocols are firstly analyzed to realize the impacts of various parameters including energy harvesting time, power splitting ratio, energy harvesting efficiency, source data rate, and the distance between the source and the relay node. Numerical results are then provided to validate the analytical findings. It is shown that the PSR outperforms the TSR at normal SNR regime in terms of throughput and ergodic rate.**

I. Introduction

Non-orthogonal multiple access (NOMA) has attracted a great attention as a promising radio access technique for future wireless networks [1]-[4]. In NOMA, many users share the same frequency and time resources. The NOMA has shown to provide a remarkably enhanced spectrum efficiency for a number of concurrent users [5]. There are three basic types including power-domain NOMA, code-domain NOMA, and hybrid power and code-domain NOMA. Specifically, the power-domain NOMA [6], [7] is considered in this work where superposition coding and successive interference cancellation (SIC) are employed at transmitter and receiver, respectively.

Energy harvesting (EH) has turned up to be vital in different wireless network models to deal with the limited power supply and storage at transceivers, such as at sensor nodes in wireless sensor networks [8]-[11]. Many EH techniques have been integrated into the devices to prolong the lifetime of energy-constrained wireless networks [12], [13]. The EH circuits can perform simultaneous wireless information and power transfer (SWIPT) which can be used in various critical environment, such as healthcare, disaster, rescue, etc. The authors in [14] and [15] investigated SWIPT based relaying networks and derived the expressions of the outage probability and ergodic capacity for amplify-and-forward and decode-and-forward (DF) relaying protocols. For the EH, both time switching based relaying (TSR) and power-splitting relaying (PSR) protocols were considered. In [16], the authors considered a SWIPT based dual-hop DF relaying network where an exact expression of the outage probability was derived.

Motivated by previous works and to fill the gap related to the researching works. In this paper, we investigate the employment of PSR and TSR protocols for SWIPT in NOMA systems. Specifically, in the PSR protocol, an energy-constrained relay node harvests a part of the energy from a source node for its own use and only uses the remaining harvested energy for information processing (IP). In the TSR protocol, the relay first spends some time for EH and then deploys the IP in the remaining time. In particular, this paper considers two transmission modes at the relay node including:

i) *Delay-limited transmission (DLT)*: In this mode, the destination node decodes the received signal block by block.
ii) *Delay-tolerant transmission (DTT)*: In this mode, the destination node can buffer the received information blocks and thus it accepts the delay due to the decoding of the received signal.

We first analyse the performance of PSR and TSR protocols in a NOMA system employing either DLT or DTT mode with DF relaying. Various performance metrics are investigated, including outage probability, throughput, and ergodic rate. The outage probabilities at both users are derived in closed-form expressions, while the throughput and ergodic rate are devised for DLT and DTT modes, respectively. It is shown than an adaptation of NOMA and SWIPT with either PSR or TSR protocol results in an enhanced outage performance for a considerably increased throughput and ergodic rate when compared to the conventional orthogonal multiple access (OMA). It also is shown that the PSR protocol has a higher throughput and ergodic rate but has a lower outage probability when compared to the TSR protocol.

II. System Model

Fig. 1 illustrates the system model under investigation, in which a source node, S, wants to transfer the information to two users D_1 and D_2. Due to an obstacle between S and D_2 as shown in Fig. 1, S first sends data to D_1, and then D_1 is exploited to assist S to forward the information to D_2. Here, D_1 employs DF relaying protocol using the energy harvested from S. The distances from S to D_1 and from D_1 to D_2 are denoted by d_1 and d_2, respectively. The complex

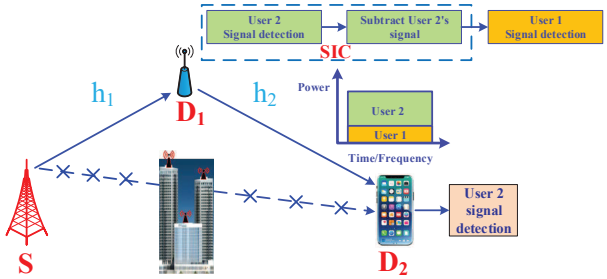

Fig. 1: System Model.

channel coefficients of $S \to D_1$ and $D_1 \to D_2$ links are denoted by h_1 and h_2, respectively, having channel gains $|h_1|^2$ and $|h_2|^2$ which are assumed to be exponentially distributed with $E[|h_1|^2] = \Omega_1^{-1}$ and $E[|h_2|^2] = \Omega_2^{-1}$. Here, E[.] denotes the expectation operation.

A. Energy Harvesting at D_1

At D_1, two EH protocols are sequentially considered, including PSR-based D_1 and TSR-based D_1.

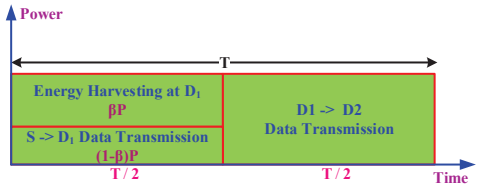

Fig. 2: PSR Protocol of Energy harvesting system.

1) Energy Harvesting at PSR-based D_1: Fig. 2 presents the communication block diagram using the PSR protocol for EH and IP at D_1 in the total time block of T. The power of the received signal at D_1 is denoted by P. It is assumed that S transmits information to D_1 in the first half of T, while the remaining time, i.e. $T/2$, is dedicated for transmitting the information from D_1 to D_2.

With the employment of superposition of the transmitted signals at S as in the NOMA scheme [17], the observed signal at D_1 is given by

$$y_{D_1} = h_1(\sqrt{a_1 P_s}x_1 + \sqrt{a_2 P_s}x_2) + n_{D_1}, \quad (1)$$

where P_s is transmission power at S, a_1 and a_2 are power allocation coefficients for data symbols x_1 and x_2 that are wished to send from S to D_1 and D_2, respectively, and n_{D_1} is an additive white Gaussian noise (AWGN) at D_1 with zero mean and variance σ^2. It is assumed that $E[x_1^2] = E[x_2^2] = 1$. Due to D_1 is closer to S than D_2, more power should be allocated to D2, i.e. $a_2 > a_1 > 0$ satisfying $a_1 + a_2 = 1$.

Employing PSR protocol, D_1 splits the received power into two parts including: i) harvested energy and ii) information processing energy. Let β, $0 < \beta < 1$, denotes the power splitting ratio. The energy harvested at D_1 can be obtained as

$$E_H^{PSR} = \beta\eta|h_1|^2\rho\,(T/2), \quad (2)$$

where $\rho \triangleq \frac{P_s}{\sigma^2}$ represents the transmit signal-to-noise ratio (SNR) and $0 < \eta < 1$ depicts the EH efficiency at the energy receiver which depends on rectifier and EH circuitry deloyed at D_1.

A part of the harvested energy is consumed at D_1 while the remaining harvested energy is used to DF the received signal to D_2. From the harvested energy E_H^{PSR}, the transmission power at D_1 can be given by

$$P_r^{PSR} = \frac{E_H^{PSR}}{(T/2)} = \frac{\beta\eta|h_1|^2\rho\,(T/2)}{(T/2)} = \beta\eta|h_1|^2\rho. \quad (3)$$

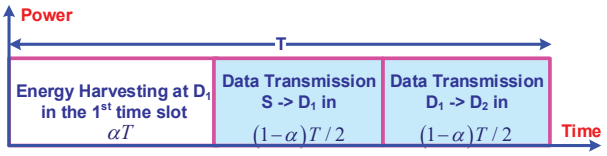

Fig. 3: TSR Protocol of Energy harvesting system.

2) Energy Harvesting at TSR-based D_1: Fig. 3 presents the TSR protocol of Energy harvesting system. T is the total block time that information is transmitted from S to D_2, and $0 < \alpha < 1$ is the fraction of the block time that D_1 harvests energy from S. The first sub-block of time, αT, is used for EH. The remaining block time, i.e. $(1-\alpha)T$, is for the information transmission, half of which, i.e. $(1-\alpha)T/2$, is used for the data transmission from S to D_1, and then the remaining time is for transmitting data from D_1 to D_2. The harvested energy at D_1 can be obtained as

$$E_H^{TSR} = \alpha\eta|h_1|^2\rho T, \quad (4)$$

From the harvested energy E_H^{TSR}, the normalized transmission power at the D_1 is given by

$$P_r^{TSR} = \frac{E_H^{TSR}}{(1-\alpha)T/2} = \frac{\alpha\eta|h_1|^2\rho T}{(1-\alpha)T/2} = \frac{2\alpha\eta|h_1|^2\rho}{(1-\alpha)}. \quad (5)$$

From (1) the received signal to interference plus noise ratio (SINR) at D_1 to detect x_2 of D_2 is given by

$$\gamma_{D_2 \to D_1} = \frac{\psi_I|h_1|^2 a_2\rho}{\psi_I|h_1|^2 a_1\rho + 1}, \quad (6)$$

where ψ_I denotes the IP coefficient in the PSR and the TSR protocols and

$$\psi_I = \begin{cases} (1-\beta)\,\eta, & for\ \ PSR. \\ \frac{(1-\alpha)}{2}\eta, & for\ \ TSR. \end{cases} \quad (7)$$

B. Information Processing at D_1 and D_2

After receiving the signal from S, D_1 decodes the signal x_2 and decodes its own signal x_1 by employing SIC [18].

After SIC, there is no interference remaining in the received signal at D_1.

The received SNR at D_1 to detect its own message x_1 is thus given by

$$\gamma_{D_1} = \psi_I|h_1|^2 a_1\rho, \quad (8)$$

Then, the decoded signal x_2 at D_1 is forwarded to D_2. The received signal at D_2 can be expressed as

$$y_{D_2} = \left(\sqrt{P_r^X} x_2\right) h_2 + n_{D_2}, \tag{9}$$

where $X \in \{PSR, TSR\}$. Then, substituting (3) and (5) into (8) , we obtain

$$y_{D_2} = (\sqrt{\psi_E \rho})\, h_1 h_2 x_2 + n_{D_2}, \tag{10}$$

where ψ_E denotes the EH coefficient in the PSR and the TSR protocols and

$$\psi_E = \begin{cases} \beta\eta, & for\ \ PSR. \\ \frac{2\alpha\eta}{(1-\alpha)}, & for\ \ TSR. \end{cases} \tag{11}$$

The received *SNR* at D_2 is therefore given by

$$\gamma_{2,D_2} = |h_2|^2 |h_1|^2 \psi_E \rho. \tag{12}$$

III. PERFORMANCE ANALYSIS OF PSR PROTOCOL

A. Outage Performance

1) Outage Probability at D_1: In the NOMA protocol, D_1 is not in outage when it can decode both x_1 and x_2 received from S. Therefore, the outage probability at D_1 can be expressed by

$$P_{D_1,PSR} = 1 - \Pr\left(\gamma_{D_2 \to D_1} > \gamma_{th_2}, \gamma_{D_1} > \gamma_{th_1}\right), \tag{13}$$

where $\gamma_{th_1} = 2^{2R_1} - 1$ and $\gamma_{th_2} = 2^{2R_2} - 1$. Here, R_1 and R_2 are the target rates for detecting x_1 and x_2, respectively, at D_1. We have the following finding of the outage probability at D_1.

Theorem 1. *The outage probability at D_1 of PSR protocol is given by*

$$P_{D_1,PSR} = 1 - e^{-\frac{\theta_{1,PSR}}{\Omega_1}}, \tag{14}$$

where $\theta_{1,PSR} = \max(\tau_{1,PSR}, \nu_{1,PSR})$, $\tau_{1,PSR} = \frac{\gamma_{th2}}{\rho \psi_I^{PSR}(a_2 - a_1\gamma_{th2})}$ *and* $\nu_{1,PSR} = \frac{\gamma_{th1}}{a_1 \psi_I^{PSR} \rho}$ *with* $a_2 > a_1\gamma_{th2}$.

Proof: The outage probability at D_1 can be computed by

$$\begin{aligned} P_{D_1,PSR} &= 1 - P_r\left(|h_1|^2 \geq \theta_{1,PSR}\right) \\ &= 1 - \textstyle\int_{\theta_{1,PSR}}^{\infty} f_{|h_1|^2}(y)\, dy = 1 - e^{-\frac{\theta_{1,PSR}}{\Omega_1}}. \end{aligned} \tag{15}$$

The proof is completed. ■

2) Outage Probability at D_2: Similarly, the outage at D_2 occurs when D_1 cannot detect x_2 to forward to D_2 or D_1 can detect x_2 but D_2 cannot recover x_2.
The outage probability at D_2 is thus given by

$$P_{D_2,PSR} = \Pr\left(\gamma_{D_2 \to D_1} < \gamma_{th_2}\right) + \Pr\left(\gamma_{2,D_2} < \gamma_{th_2}, \gamma_{D_2 \to D_1} > \gamma_{th_2}\right) \tag{16}$$

Theorem 2. *The outage probability at D_2 of PSR protocol can be computed by*

$$P_{D_2,PSR} = 1 - e^{-\frac{\tau_{1,PSR}}{\Omega_1}} + \int_{\tau_{1,PSR}}^{\infty} \left(1 - e^{\frac{-\gamma_{th_2}}{x\psi_E^{PSR}\rho\Omega_2}}\right) \frac{1}{\Omega_1} \exp\left(\frac{-x}{\Omega_1}\right) dx \tag{17}$$

Proof: From (16), we have

$$\begin{aligned} P_{D_2,PSR} = &\underbrace{P_r\left(|h_1|^2 < \tau_{1,PSR}\right)}_{J_2} + \\ &\underbrace{P_r\left(|h_1|^2 > \tau_{1,PSR}, |h_2|^2 < \frac{\gamma_{th_2}}{|h_1|^2 \psi_E^{PSR} \rho}\right)}_{J_3} \end{aligned} \tag{18}$$

where J_2 and J_3 can be computed by

$$J_2 = \textstyle\int_0^{\tau_{1,PSR}} f_{|h_1|^2}(x)\, dx = 1 - e^{-\frac{\tau_{1,PSR}}{\Omega_1}} \tag{19}$$

$$J_3 = \int_{\tau_{1,PSR}}^{\infty} \frac{1}{\Omega_1} \left[1 - \exp\left(\frac{-\gamma_{th_2}}{x\psi_E^{PSR}\rho\Omega_2}\right)\right] \exp\left(\frac{-x}{\Omega_1}\right) dx \tag{20}$$

Substituting (19) and (20) into (18), the theorem is proved. ■

B. Throughput for Delay-limited Transmission Mode

In DLT mode, S transmits information with a constant rate of R, depending on the performance of the outage probability due to wireless fading channels. The total system throughput of the PSR protocol in the DLT mode is given by

$$\tau_{t,PSR} = (1 - P_{D_1,PSR}) R_1 + (1 - P_{D_2,PSR}) R_2, \tag{21}$$

where $P_{D_1,PSR}$ and $P_{D_2,PSR}$ can be obtained from (12) and (13), respectively. Here, R_1 and R_2 are the target rates for detecting x_1 and x_2, respectively, at D_1.

C. Ergodic Rate for Delay-tolerant Transmission Mode

In DTT mode, the throughput is determined by evaluating the ergodic rate at D_1 and D_2.

1) Ergodic Rate at D_1: For the case when D_1 can detect x_2, the achievable rate of D_1 can be written as

$$R_{D_1,PSR} = \frac{1}{2} \log_2\left(1 + \gamma_{D_1}\right). \tag{22}$$

Theorem 3. *The ergodic rate at PSR-based D_1 in DTT mode is given by*

$$R_{D_1,PSR} = \frac{-\exp\left(\frac{1}{\psi_I^{PSR} a_1 \rho \Omega_1}\right)}{2\ln 2} Ei\left(\frac{-1}{\psi_I^{PSR} a_1 \rho \Omega_1}\right), \tag{23}$$

where $Ei(x)$ denotes the exponential integral function [19, $Eq.(3.352.4)$].

Proof: See Appendix 1. ■

2) Ergodic Rate at D_2: Since x_2 needs to be detected at both D_1 and D_2, the achievable rate at D_2 in DTT mode with PSR protocol can be written as

$$R_{D_2,PSR} = \frac{1}{2} \log_2\left(1 + \min\left(\gamma_{D_2 \to D_1}, \gamma_{2,D_2}\right)\right). \tag{24}$$

Theorem 4. *The ergodic rate at D_2 of the PSR protocol in DTT mode is given by*

$$R_{D_2,PSR} = \tfrac{1}{2\ln 2} \textstyle\int_0^{\frac{a_2}{a_1}} \frac{A}{1+x} dx, \tag{25}$$

where

$$A = e^{-\frac{x}{\psi_I^{PSR}\rho(a_2-a_1x)\Omega_1}} + \int_{\frac{x}{\psi_I^{PSR}\rho(a_2-a_1x)}}^{\infty} \frac{1}{\Omega_1}\left(1-e^{-\frac{x}{y\rho\psi_E^{PSR}\Omega_2}}\right)e^{-\frac{y}{\Omega_1}}dy \quad (26)$$

Proof: See Appendix 2. ■

3) Ergodic rate of the system: The ergodic rate of the NOMA system employing PSR protocol in DTT mode is given by

$$\tau_{r,PSR} = R_{D_1,PSR} + R_{D_2,PSR}, \quad (27)$$

where $R_{D_1,PSR}$ and $R_{D_2,PSR}$ can be obtained from (23) and (25), respectively.

IV. PERFORMANCE ANALYSIS OF TSR PROTOCOL

A. Outage performance

Similarly, the outage probabilities at D_1 and D_2 of TSR protocol are derived as in the following theorems.

Theorem 5. *The outage probability at D_1 of TSR protocol is given by*

$$P_{D_1,PSR} = 1 - e^{-\frac{\theta_{1,TSR}}{\Omega_1}}, \quad (28)$$

where $\theta_{1,TSR} = \max(\tau_{1,TSR}, \nu_{1,TSR})$, $\tau_{1,TSR} = \frac{\gamma_{th2}}{\rho\psi_I^{TSR}(a_2-a_1\gamma_{th2})}$ *and* $\nu_{1,TSR} = \frac{\gamma_{th1}}{a_1\psi_I^{TSR}\rho}$ *with* $a_2 > a_1\gamma_{th2}$.

Proof: The proof is similar to that of Theorem 1 where ψ_I in the TSR protocol is given by (7) ■

Theorem 6. *The outage probability at D_2 can be given by*

$$P_{D_2,TSR} = 1 - e^{-\frac{\tau_{1,TSR}}{\Omega_1}} + \int_{\tau_{1,TSR}}^{\infty}\left(1-\mathrm{e}^{\frac{-\gamma_{th_2}}{x\psi_E^{TSR}\rho\Omega_2}}\right)\frac{1}{\Omega_1}\exp\left(\frac{-x}{\Omega_1}\right)d\mathrm{x}. \quad (29)$$

Proof: The proof is similar to that of Theorem 2 where ψ_I and ψ_E in the TSR protocol are given by (7) and (11) ■

B. Throughput for Delay-limited Transmission Mode

Total system throughput of HD transmission mode in the NOMA system is given by

$$\tau_{t,TSR} = (1 - P_{D_1,TSR})R_1 + (1 - P_{D_2,TSR})R_2 \quad (30)$$

where $P_{D_1,TSR}$ and $P_{D_2,TSR}$ can be obtained from (28) and (29), respectively.

C. Ergodic Rate for Delay-tolerant Transmission Mode

1) Ergodic Rate at D1: For the case where D_1 can detect x_2, the achievable rate at D_1 can be written as

$$R_{D_1,TSR} = \frac{1}{2}\log_2(1+\gamma_{D_1}). \quad (31)$$

Theorem 7. *The ergodic rate at D_1 for HD NOMA is given by*

$$R_{D_1,TSR} = \frac{-\exp\left(\frac{1}{\psi_I^{TSR}a_1\rho\Omega_1}\right)}{2\ln 2}Ei\left(\frac{-1}{\psi_I^{TSR}a_1\rho\Omega_1}\right) \quad (32)$$

Proof: The proof is similar to that of Theorem 3 where ψ_I in the TSR protocol is given by (7) ■

2) Ergodic Rate at D2: The achievable rate at D_2 for HD transmission mode in the NOMA system can be written as

$$R_{D_2,TSR} = \frac{1}{2}\log_2(1+\min(\gamma_{D_2\to D_1}, \gamma_{2,D_2})). \quad (33)$$

Theorem 8. *The ergodic rate at D_2 is given by*

$$R_{D_2,TSR} = \frac{1}{2\ln 2}\int_0^{\frac{a_2}{a_1}}\frac{B}{1+x}d\mathrm{x}, \quad (34)$$

where

$$B = e^{-\frac{x}{\psi_I^{TSR}\rho(a_2-a_1x)\Omega_1}} + \int_{\frac{x}{\psi_I^{TSR}\rho(a_2-a_1x)}}^{\infty}\frac{1}{\Omega_1}\left(1-e^{-\frac{x}{y\rho\psi_E^{TSR}\Omega_2}}\right)e^{-\frac{y}{\Omega_1}}dy \quad (35)$$

Proof: The proof is similar to that of Theorem 4 where ψ_I and ψ_E in the TSR protocol are given by (7) and (11) ■

D. Ergodic rate of the system

The system ergodic rate of HD transmission mode in the NOMA system can be determined by

$$\tau_{r,TSR} = R_{D_1,TSR} + R_{D_2,TSR} \quad (36)$$

where $R_{D_1,TSR}$ and $R_{D_2,TSR}$ can be obtained from (32) and (34), respectively.

V. SIMULATION RESULTS

In this section, we use Matlab simulation to prove provided results and confirm our analytical expressions contained in the preceding sections.

Without loss of generality, we assume that the distance between S and D_2 is normalized to unity, i.e. $\Omega_{SD_2} = 1, \Omega_{SD_1} = d^{-m}$ and $\Omega_{D_1D_2} = (1-d)^{-m}$, where d is the normalized distance between the S and D_1 setting to be $d = 0.3$ and m is pathloss exponent setting to be $m = 2$. The power allocation coefficients of NOMA are $a_1 = 0.2$ and $a_2 = 0.8$ for D_1 and D_2, respectively. The target rates are set as $R_1 = 2$ bps and $R_2 = 1$ bps.

The first work we consider is evaluating the outage probability of the system. Specifically, Figure 4 and Figure 5 illustrate the outage probability of two users for the PSR protocol versus SNR, β and α respectively. It can be observed that User 2 has a lower outage probability than that of User 1 in the HD NOMA scheme as well as in the HD OMA scheme. Also, the outage probability of two users in the HD NOMA scheme is shown to be lower than those in the HD OMA scheme and TSR protocol has the outage probability higher PSR protocol. Specifically, Figure 4 illustrates the outage probability of two users for the PSR and the TSR protocols versus SNR with ρ.

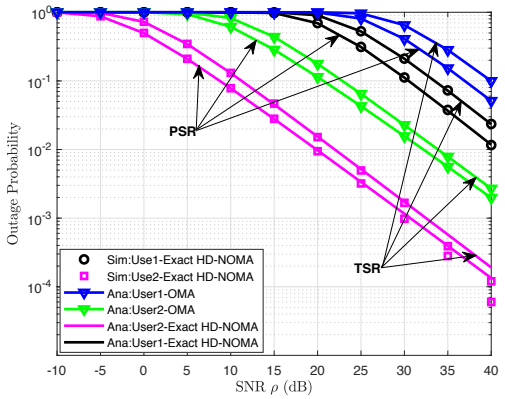

Fig. 4: Outage probability versus transmitting SNR.

Figure 5 plots the outage probability of two users for the PSR and the TSR protocols versus SNR with $\beta = \alpha$. The exact theoretical curves for the outage probability of two users in Figure 4 and Figure 5 for HD NOMA are plotted according to (13), (14), (15), (16), (17), (18), (19), (20), (28), (29), respectively.

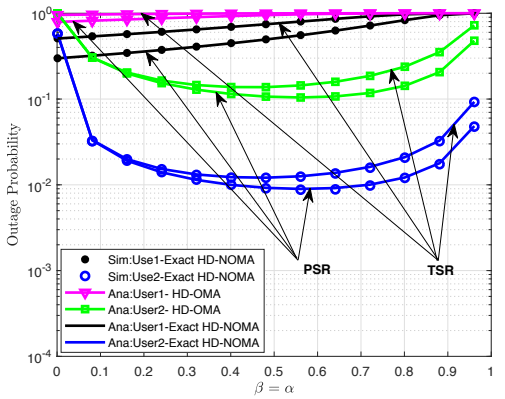

Fig. 5: Outage probability versus the energy harvesting coefficients.

Figure 6 and Figure 7 plot throughput and the ergodic rate of two users for the PSR and the TSR protocols versus SNR with $\beta = \alpha$. The exact theoretical curves for the ergodic rate of two users for HD NOMA are plotted according to (21), (22), (23), (24), (25), (27), (30), (31), (32), (33), (34), (35) and (36), respectively.

VI. CONCLUSION

In this paper, we have studied HD user the PSR and the TSR protocols for wireless EH and IP. We have used a DF relaying network with two cooperative relaying protocol were the PSR and the TSR. The closed-form expressions of outage probability and ergodic rate for two users have derived. Based on our analytical results, it shows that the PSR protocol has outperformed performance than the TSR protocol. Furthermore, the expression of the achievable throughput,

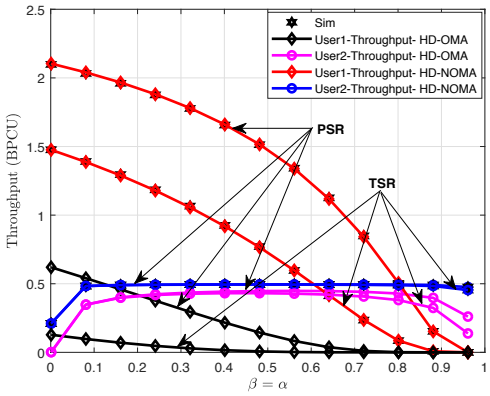

Fig. 6: The throughput of two users for the PSR and the TSR protocols versus $\beta = \alpha$.

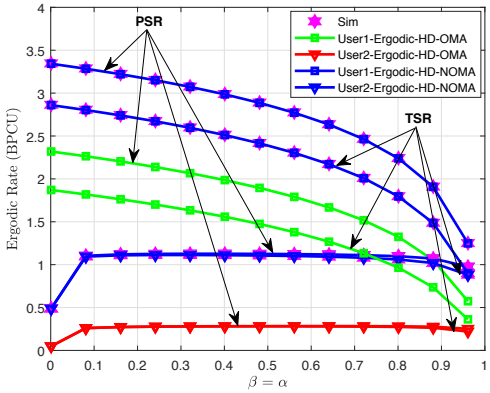

Fig. 7: The ergodic rate of two users for the PSR and the TSR protocols versus $\beta = \alpha$.

ergodic sum rate for HD user the PSR and the TSR protocols for wireless EH, and IP also were derived.

VII. APPENDICES

A. Appendix 1 - Proof of Theorem 3

The ergodic rate at D_1 can be written as

$$R_{D_1,PSR} = \frac{1}{2}\mathrm{E}\left[\log_2\left(1+\psi_I^{PSR}|h_1|^2 a_1\rho\right)\right] = \frac{1}{2\ln 2}\int_0^\infty \frac{1-F_X(x)}{1+x}dx \tag{37}$$

The cumulative distribution function (CDF) of X is calculated as

$$\begin{aligned} F_X(x) &= \Pr\left(|h_1|^2 < \frac{x}{\psi_I^{PSR}a_1\rho}\right) = \int_0^{\frac{x(z\rho+1)}{\psi_I^{PSR}a_1\rho}} \frac{1}{\Omega_1}e^{-\frac{y}{\Omega_1}}dy \\ &= 1-e^{-\frac{x}{\psi_I^{PSR}a_1\rho\Omega_1}} \end{aligned} \tag{38}$$

By replacing (36) in (35), the ergodic rate at D_1 can be derived as

$$\begin{aligned} R_{D_1,PSR} &= \frac{1}{2}\frac{1}{\ln 2}\int_0^\infty \frac{1}{1+x}e^{-\frac{x}{\psi_I^{PSR}a_1\rho\Omega_1}}dx \\ &= \frac{-\exp\left(\frac{1}{\psi_I^{PSR}a_1\rho\Omega_1}\right)}{2\ln 2}Ei\left(\frac{-1}{\psi_I^{PSR}a_1\rho\Omega_1}\right) \end{aligned}$$

We can derive (23). The proof is completed.

B. Appendix 2 - Proof of Theorem 4

The proof begins by giving the ergodic rate at D_2 as follows

$$R_{D_2,PSR} = E\left[\frac{1}{2}\log_2\left(1+\underbrace{\min\left(\gamma_{D_2\to D_1},\gamma_{2,D_2}\right)}_{J_1}\right)\right]$$

$$J_1 = \underbrace{\min\left(\frac{\psi_I^{PSR}|h_1|^2 a_2\rho}{\psi_I^{PSR}|h_1|^2 a_1\rho+1}, |h_2|^2|h_1|^2\psi_E^{PSR}\rho\right)}_{X}$$

The CDF of X is calculated as follows

$$F_X(x) = I_3 + I_4 \tag{39}$$

where

$$I_3 = \Pr\left(\frac{\psi_I^{PSR}|h_1|^2 a_2\rho}{\psi_I^{PSR}|h_1|^2 a_1\rho+1} < |h_2|^2|h_1|^2\psi_E^{PSR}\rho, \frac{\psi_I^{PSR}|h_1|^2 a_2\rho}{\psi_I^{PSR}|h_1|^2 a_1\rho+1} < x\right)$$

$$= U\left(\frac{a_2}{a_1}-x\right)\int_0^{\frac{x}{\psi_I^{PSR}\rho(a_2-a_1x)}} \frac{1}{\Omega_1} e^{-\frac{\psi_I^{PSR}a_2}{\left(\psi_I^{PSR}ya_1\rho+1\right)\psi_E^{PSR}\Omega_2}-\frac{y}{\Omega_1}}dy \tag{40}$$

and

$$I_4 =$$

$$\Pr\left(\frac{\psi_I^{PSR}|h_1|^2 a_2\rho}{\psi_I^{PSR}|h_1|^2 a_1\rho+1} > |h_2|^2|h_1|^2\psi_E^{PSR}\rho, |h_2|^2|h_1|^2\psi_E^{PSR}\rho < x\right)$$

$$= \int_0^{\frac{x}{\psi_I^{PSR}\rho(a_2-a_1x)}} \frac{1}{\Omega_1}\left(1-e^{-\frac{\psi_I^{PSR}a_2}{\left(\psi_I^{PSR}ya_1\rho+1\right)\psi_E^{PSR}\Omega_2}}\right)e^{-\frac{y}{\Omega_1}}dy$$

$$= \int_{\frac{x}{\psi_I^{PSR}\rho(a_2-a_1x)}}^{\infty} \frac{1}{\Omega_1}\left(1-e^{-\frac{y}{y\rho\psi_E^{PSR}\Omega_2}-\frac{y}{\Omega_1}}\right)dy. \tag{41}$$

The CDF of X is given by

$$F_X(x) = U\left(\frac{a_2}{a_1}-x\right)\left[1-e^{-\frac{x}{\psi_I^{PSR}\rho(a_2-a_1x)\Omega_1}} + \int_{\frac{x}{\psi_I^{PSR}\rho(a_2-a_1x)}}^{\infty}\frac{1}{\Omega_1}\left(1-e^{-\frac{x}{y\rho\psi_E^{PSR}\Omega_2}}\right)e^{-\frac{y}{\Omega_1}}dy\right]. \tag{42}$$

where $U(x)$ is unit step function. By replacing (42) into (24), we can obtain (25). The proof is completed.

REFERENCES

[1] L. Dai, B. Wang, Y. Yuan, S. Han, I. Chih-Lin, and Z. Wang, "Non-orthogonal multiple access for 5g: solutions, challenges, opportunities, and future research trends," *IEEE Commun. Maga.*, vol. 53, no. 9, pp. 74-81, 2015.

[2] H. Q. Tran, P. Q. Truong, C. V. Phan, and Q.-T. Vien, "On the energy efficiency of NOMA for wireless backhaul in multi-tier heterogeneous CRAN," *in Proc. SigTelCom*, Da Nang, 2017. Vietnam, January 2017, pp. 229234.

[3] N. Bhuvanasundaram, H. X. Nguyen, R. Trestian, and Q.-T. Vien, "Non-orthogonal multiple access schemes for next-generation 5G networks: A survey. In: 5G Radio Access Networks: Centralized RAN, Cloud-RAN and Virtualization of Small Cells," *CRC Press*, pp. 51-66, ISBN 9781498747103, 2017.

[4] H. Q. Tran, C. V. Phan, and Q.-T. Vien, "An overview of 5G technologies. In: Emerging Wireless Communication & Network Technologies: Principle, Paradigm and Performance, " *Springer*, pp. 59-80, ISBN 9789811303951, 2018.

[5] S. R. Islam, N. Avazov, O. A. Dobre, and K. S. Kwak, "Power domain non-orthogonal multiple access (NOMA) in 5G systems: Potentials and challenges," *IEEE Commun. Surveys & Tutorials*, vol. 19, no. 2, pp. 721-742, 2017.

[6] K. Higuchi and A. Benjebbour, "Non-orthogonal multiple access (noma) with successive interference cancellation for future radio access," *IEICE Trans. Commu.*, vol. 98, no. 3, pp. 403-414, 2015.

[7] T. M. Hoang, N. T. Tan, N. H. Hoang, and P. T. Hiep, "Performance analysis of decode-and-forward partial relay selection in NOMA systems with RF energy harvesting," *Wireless Networks*, pp. 1-11, May. 2018.

[8] P. T. Venkata, S. N. A. U. Nambi, R. V. Prasad, and I. Niemegeers, "Bond graph modeling for energy-harvesting wireless sensor networks," *IEEE Computer Society*, vol. 45, no. 9, pp. 31-38, Sep. 2012.

[9] B. Medepally and N. B. Mehta, "Voluntary energy harvesting relays and selection in cooperative wireless networks," *IEEE Trans. Wireless Commun.*, vol. 9, no. 11, pp. 3543-3553, Nov. 2010.

[10] L. Mateu and F. Moll, "Review of energy harvesting techniques and applications for microelectronics," *in Proc. SPIE Circuits and Syst. II*, pp. 359-373, 2005.

[11] S. Sudevalayam and P. Kulkarni, "Energy harvesting sensor nodes: Survey and implications," *IEEE Commun. Surveys Tuts.*, vol. 13, no. 3, pp. 443-461, 2011.

[12] D. Wang, Y. Li, Y. Ye et al., "Joint time allocation and power splitting schemes for df energy harvesting relaying networks," *in Proc. IEEE 86nd Vehicular Tech. Conf.*, to appear, pp. 1-5, 2017.

[13] C. K. Ho and R. Zhang, "Optimal energy allocation for wireless communications with energy harvesting constraints," *IEEE Trans. Signal Process.*, vol. 60, no. 9, pp. 4808-4818, 2012.

[14] A. A. Nasir, X. Zhou, S. Durrani, and R. A. Kennedy, "Relaying protocols for wireless energy harvesting and information processing," *IEEE Trans. Wireless Commun.*, vol. 12, no. 7, pp. 3622-3636, 2013.

[15] Y. Gu and S. Assa, "RF-based energy harvesting in decode-and-forward relaying systems: Ergodic and outage capacities," *IEEE Trans. Wireless Commun.*, vol. 14, no. 11, pp. 6425-6434, 2015.

[16] F. Wang, W. Xu, S. Li, Z. Feng, and J. Lin, "Outage probability analysis of DF relay networks with RF energy harvesting," *in Proc. IEEE Global Commun. Conf.*, pp. 1-5, 2015.

[17] Y. Wang, B. Ren, S. Sun, S. Kang, and X. Yue, "Analysis of Non-Orthogonal Multiple Access for 5G," *China Commun.*, vol. 13, no.Supplement No. 2, pp. 52-66, 2016.

[18] S. Luo, R. Zhang, and T. J. Lim, "Optimal save-then-transmit protocol for energy harvesting wireless transmitters," *Transactions on Wireless Communications*, vol. 13, no. 3, pp. 1196-1207, 2013.

[19] Gradshteyn, I.S., Ryzhik, I.M, "Table of integrals, series and products," *Academic, San Diego, CA*, 6th edn, 2000.